ChemComm

ROYAL SOCIETY OF CHEMISTRY

COMMUNICATION

Cite this: *Chem. Commun.*, 2020, **56**, 2280

Received 17th December 2019,
Accepted 20th January 2020

DOI: 10.1039/c9cc09796a

rsc.li/chemcomm

Fsp^3-rich and diverse fragments inspired by natural products as a collection to enhance fragment-based drug discovery†

Abigail R. Hanby,[a] Nikolaj S. Troelsen,[ab] Thomas J. Osberger,[ac] Sarah L. Kidd,[ad] Kim T. Mortensen[a] and David R. Spring*[a]

Herein, we describe the natural product inspired synthesis of 38 complex small molecules based upon 20 unique frameworks suitable for fragment-based screening. Utilising an efficient strategy, two key building block diastereomers were harnessed to generate novel, three-dimensional fragments which each possess numerous synthetically accessible fragment growth positions.

Within the last two decades fragment-based drug discovery (FBDD) has evolved into a mainstream approach to deliver high-quality leads for both routine and challenging biological targets.[1,2] The fundamental strategy behind FBDD relies on the identification of very small and often weak binders during screening, which are later grown into strongly binding leads. Hence, organic synthesis plays a vital role in this process to enable sufficient fragment elaboration. However, in an analogous fashion to high-throughput screening collections, within recent years deficiencies in FBDD collections have emerged relating to lack of functional handles and suitability for fragment growth without significant synthetic exploration. As a result, novel fragments with these features are urgently required to augment existing commercial collections. In particular there is a need for fragments containing polar functionalities for fragment growth and biological recognition.[3]

Whilst complex fragments have been well-debated within the literature,[4] importantly increased sp^3-content increases both the number and range of accessible fragment growth vectors,[3] thus enabling efficient elaboration of fragment hits in a three-dimensional (3D) manner. Compounds featuring a high fraction of sp^3 centres (Fsp^3) have also been shown to increase the likelihood of progression through the development phases of drug discovery.[5,6] Furthermore, inherently these compounds are also more 3D and fragments of this nature also provide tools to interrogate challenging biological targets.[7] This has led to the development of numerous 3D fragment libraries.[8] One such strategy to incorporate these features is the introduction of all-carbon quaternary stereocentres. These motifs are of significant interest due to their presence in numerous natural products (NPs) and marketed drugs, as well as their ability to confer greater three-dimensionality, novelty and metabolic stability.[9] However, despite notable advances in the synthesis of these stereocentres their construction remains a major challenge due to their congested nature and conformational restriction,[10] and thus rarely feature in fragment collections.

NPs have proven a long-standing source of bioactive molecules and have enabled the investigation and manipulation of many biological systems,[11] yet due to their size often remain unsuitable for FBDD. More recently, however, NP-derived fragments have been reported through algorithmic fragmentation,[7] suggesting their inherent structural complexity can be harnessed to deliver novel fragment libraries. As a complimentary strategy, we hypothesised that a library of diverse, sp^3-rich fragments with high NP-likeness could be designed, whilst maintaining FBDD suitability through control of the physicochemical properties.

To achieve this, we envisaged the exploitation of a stereochemically-rich and densely functionalised building block (**1**) through a divergent synthetic scheme (Fig. 1). 2,2-Disubstituted-cycloketone/cycloalcohol motifs are considered privileged scaffolds due to their presence within a number of drugs and NPs.[12] As such incorporation of this core within a novel fragment library would be of particular interest. Indeed, use of building block **1**, containing multiple synthetic handles and vicinal stereocentres, would also enable the installation of complexity to the resulting library members through stereochemical enrichment.

Accordingly, synthesis of key precursors *syn*-**1** and *anti*-**1** commenced from the commercially available cyclopentanedione **2**, which could then be readily alkylated to form **3** (Scheme 1). Subsequent reductive desymmetrisation by $NaBH_4$ resulted in a separable mixture of diastereomers *anti*-**1** and *syn*-**1**. A racemic strategy was employed to enable downstream screening of both enantiomers.[13] Moreover, to exemplify the versatility of

[a] *Department of Chemistry, University of Cambridge, Lensfield Rd, Cambridge, UK. E-mail: spring@ch.cam.ac.uk*
[b] *Center for Nanomedicine and Theranostics, Department of Chemistry, Technical University of Denmark (DTU), Denmark*
[c] *Department of Chemistry, California State Polytechnic University, Pomona, USA*
[d] *School of Chemistry, University of Leeds, Woodhouse Lane, Leeds, UK*

† Electronic supplementary information (ESI) available. See DOI: 10.1039/c9cc09796a

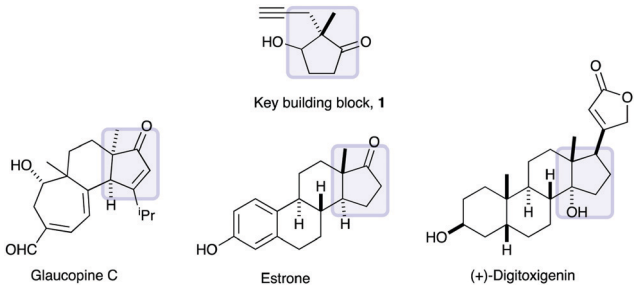

Fig. 1 Natural products synthesised from 3-hydroxy-2,2-disubstituted-cyclopentan-1-ones (highlighted in blue).

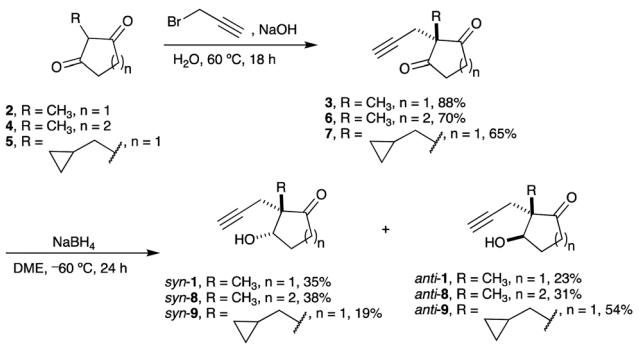

Scheme 1 Synthesis of cyclisation precursors.

this building block both the R substituent and the ring size were altered to demonstrate potential for fragment elaboration and analogue synthesis.

Our initial investigations began with building block *anti*-**1**. To prevent side reactions, temporary TBS protection of the hydroxyl group was found to be necessary for transformations not involving this functional group (Scheme 2). TBAF-mediated deprotection could then be employed as the last step in each sequence to reveal the final scaffolds (Scheme 2). Firstly, *anti*-**1** was initially derivatised through exploitation of the acidic position α to the ketone. Mono-alkylation at this position and subsequent ring closing enyne metathesis (RCEYM) furnished bridged scaffold **10**. Alternatively, α-methylenation of *anti*-**1** enabled [3+2] cycloaddition reactions to be explored, thus forming spirocyclic products **12**, **13a** and **13b** through cyclisation with either an *in situ* generated nitrone or azomethine ylide, respectively. In a similar fashion, IBX-mediated dehydrogenation reaction was employed to afford the enone intermediate **14**. Subsequent TFA promoted cycloaddition afforded the [5,5]-*cis*-fused bicyclic scaffolds **15a** and **15b**, again *via* an azomethine ylide.

To expand the exploitable functionality within *anti*-**1** the ketone was next modified. Indeed, **16** was synthesised from *anti*-**1** in two steps, whereupon RCEYM and deprotection was employed to furnish diene **17**. It was further found that subjecting **16** to Pauson–Khand cyclisation conditions afforded the separable diastereomers **18a** and **18b** featuring a [5,6,5]-ring system.

Next, Beckmann rearrangement of TBS-protected *anti*-**1** yielded **19** as a single regioisomer, which upon simple deprotection furnished lactam **20**. The alkyne handle within **19** also provided the opportunity to generate a further three scaffolds. Firstly, through allylation followed by Pauson–Khand cyclisation to form **21**, and RCEYM to form diene **22**, or derivatisation of **19** to the vinyl-iodide followed by cyclisation with the amide to give **23**. Finally, the terminal alkyne functionality was also modified directly from *anti*-**1** *via* base-induced cycloaddition with α-chlorobenzaldoxime to afford the isoxazole **24**.

In an analogous fashion, the utility of *syn*-**1** was next investigated. Firstly, the terminal alkyne was once more modified, however in this case utilising a Ru-catalysed azide-alkyne cycloaddition (RuAAC) to afford **25**.

Subsequently, the utility of the hydroxyl functionality for forming additional scaffolds was explored. Firstly, mesylation of the hydroxyl group within *syn*-**1** allowed the introduction of a nitrile group *via* substitution with KCN, which proceeded with overall retention of configuration. The relative arrangement between the nitrile group and the quaternary carbon was deduced by NOE correlation analysis of both nitriles *syn*-**26** and *anti*-**26** and is consistent with similar observations.[14] With the continued aim to access diverse scaffolds, subjection of this intermediate to cobalt-catalysed [2+2+2] cyclotrimerisation conditions afforded tricyclic pyridine **27**.

In addition to direct use of the hydroxyl it was envisioned that the introduction of additional functional handles could be achieved *via* exploitation of the nucleophilicity of the OH. Indeed, initial Michael addition of *syn*-**1** to ethyl propiolate gave **28**, which upon subjection to tributyltin-mediated radical cyclisation and subsequent acidic destannylation was transformed to give the *exo*-ene [6,5]-scaffold **29**. In a similar fashion, esterification of the free hydroxyl in *syn*-**1** with either azido- or alkene-containing coupling partners afforded compounds **30**–**33**. This provided the opportunity to generate several medium-sized rings. For example, RCEYM was employed for the pairing of the alkene and alkyne in **30** to form the bicyclic structure **34**, whilst bridged scaffold **35** was synthesized from **31** *via* a complexity-generating tandem cross enyne metathesis-intramolecular Diels–Alder reaction. Alternatively, intramolecular pairing of the azide and the alkyne groups in **32** and **33** *via* a RuAAC yielded 1,5-disubstituted triazoles **36** and **37**, respectively. Next, a smaller six-membered ring lactone, **38**, was synthesized *via* a Baeyer–Villiger oxidation of the ketone.

Finally, pairing reactions between the hydroxyl and alkyne groups were investigated to give fused bicyclic ring systems. In this manner, ruthenium-catalysed *endo*-pairing of the alcohol and alkyne functionalities gave **39**. Next, **40a** and **40b** were formed *via* an iridium-catalysed *exo*-cyclisation with addition of methanol, whilst palladium catalysed *exo*-cyclisation in presence of CO gave **41**.

Each fragment was synthesised from building blocks *syn*-**1** and *anti*-**1** in no more than five steps, highlighting the synthetic efficiency of the strategy described. Importantly, these scaffolds bear up to four stereocentres, including quaternary centres and spirocyclic ring systems, introducing NP-like elements to the library. In addition, each scaffold contains multiple synthetic vectors for fragment growth, including a variety of polar functionalities and alkenes to enable derivatisation. To further

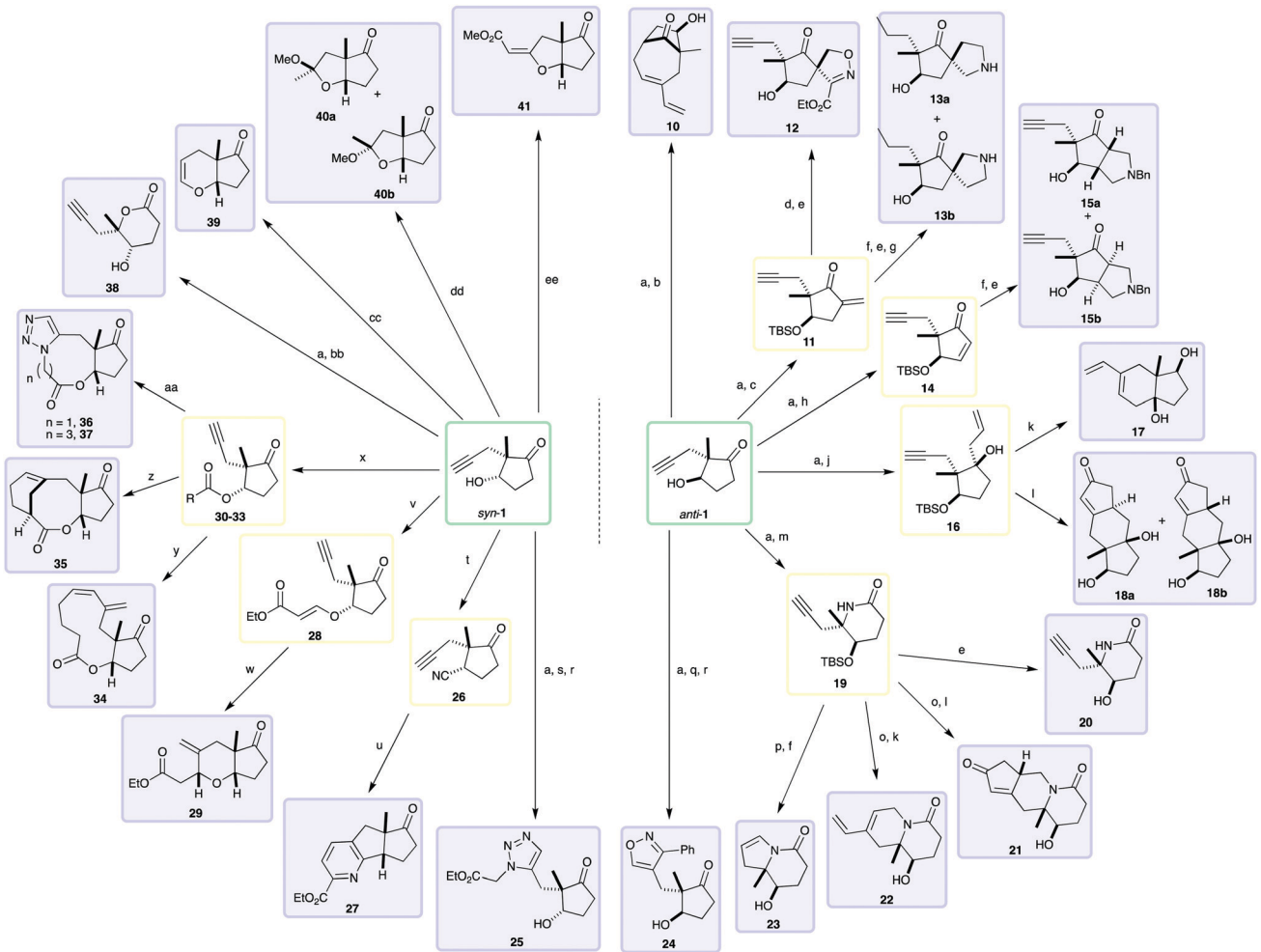

Scheme 2 (a) TBSCl, imidazole, DMF, 95–98%; (b) (i) LiHMDS, allyl bromide, THF, 76 : 24 *dr*, (ii) Hoveyda–Grubbs II, ethylene, PhMe, (iii) TBAF, THF, 13% over three steps; (c) CH_2Br_2, Et_2NH, CH_2Cl_2, 68%; (d) 1-ethyl oxalyl chloride 2-oxime, Et_3N, CH_2Cl_2, 70%; (e) TBAF, THF, 44–95%; (f) *N*-(methoxymethyl)-*N*-(trimethylsilylmethyl)benzylamine, TFA, CH_2Cl_2, 25–61%; (g) 10% Pd/C, H_2, 98–99%; (h) IBX, PhF/DMSO (2 : 1), 45%; (j) allylmagnesium bromide, THF, 75 : 25 *dr*, 62%; (k) Grubbs II, ethylene, PhMe; (ii) TBAF, THF, 66–69% over two steps; (l) (i) $Co_2(CO)_8$, CH_2Cl_2, then NMO, (ii) TBAF, THF, 17–76% over two steps; (m) *O*-(mesitylenesulfonyl)hydroxylamine, CH_2Cl_2, then $BF_3{\cdot}Et_2O$, 66%; (o) NaH, DMF, then allyl bromide, 76%; (p) (i) $InCl_3$, DIBALH, Et_3B, I_2, THF; (ii) Cs_2CO_3, CuI, *N*,*N*′-dimethylethyl-1,2-diamine, PhMe, 64%; (q) Cp*Ru(COD)Cl, α-chlorobenzaldoxime, Et_3N, DCE, 77%; (r) TBAF, AcOH, THF, 76–80%; (s) ethyl azidoacetate, $[Cp^*RuCl]_4$, PhMe, 86%; (t) (i) MsCl, pyridine, (ii) KCN, DMSO, 60% over two steps; (u) $CpCo(CO)_2$, ethyl propiolate, PhMe, 10%; (v) ethyl propiolate, NMM, CH_2Cl_2, 93%; (w) (i) Bu_3SnH, AIBN, PhMe, (ii) *p*-TsOH, CH_2Cl_2, 59% over two steps; (x) RCO_2H, DCC, DMAP, CH_2Cl_2; **30** R = $(CH_2)_3CHCH_2$, 91%, **31** R = $CHCH_2$, 51%, **32** R = CH_2N_3, 97%; **33** R = $(CH_2)_3N_3$, 84%; (y) R = $(CH_2)_3CHCH_2$, Grubbs II, ethylene, PhMe, 85%; (z) R = $CHCH_2$, Hoveyda–Grubbs II, ethylene, PhMe, 87%; (aa) R = CH_2N_3 or R = $(CH_2)_3N_3$, Cp*RuCl(cod), PhMe, 88% and 87%, respectively; (bb) (i) $KHCO_3$, *m*CPBA, CH_2Cl_2 (ii) TBAF, THF, 29% over two steps; (cc) NHS, Bu_4NPF_6, $NaHCO_3$, PPh_3, $CpRu(PPh_3)_2Cl$, DMF, 65%; (dd) $[Ir(cod)Cl]_2$, MeOH, 22 : 78 *dr*, 18% **40a** and 58% **40b**; (ee) $Pd(CH_3CN)_2Cl_2$, *p*-benzoquinone, CO, CH_2Cl_2, 33% (see ESI† for full experimental details).

demonstrate the utility of the quaternary substituent as a further growth vector and the ability to modify the ring size of the starting material, selected 6-membered ring and methylcyclopropane analogues of these scaffolds were also synthesised using *syn*-**8** and *syn*-**9**, adding a further four scaffolds to the library (see ESI†).

The control of the physicochemical properties of screening libraries underpins the FBDD strategy. Thus, calculation of a range of physicochemical properties of the compounds was conducted. This analysis demonstrates the library adheres to the 'rule of three' guidelines commonly adopted within the field (Table 1). This library also compared favourably to more recently developed complex and diverse commercial libraries.

To quantitatively assess the degree of shape diversity in the resulting library, principal moment of inertia (PMI) analysis was performed.[15] The resulting PMI plot showed that the compounds were widely dispersed, with 92% out of "flatland" (npr1 + npr2 $\leq$ 1.1) (Fig. 2).[5,17] A comparative PMI analysis of this library with the Maybridge diversity set indicated a higher level of overall molecular shape diversity and three-dimensionality was achieved with this library.

Finally, an analysis of the NP-likeness of the synthesised fragment library was also evaluated (see ESI†).[18] Satisfyingly, our library exhibited a high NP-likeness, indicating an excellent distribution in NP-like space (Fig. 3). In contrast, the commercial fragment libraries showed significantly lower resemblance to NPs.

Table 1 Mean physicochemical properties of fragment collections

Property[a]	This work	Maybridge diversity set	Life chemicals 3D	Ideal value[b]
MW	208	180	253	≤230
SlogP	1.37	1.92	1.65	≤3
HBA	2.63	2.46	2.72	≤3
HBD	0.79	0.86	1.53	≤3
Chiral centres	2.45	0.16	1.23	–
Fraction sp^3	0.70	0.29	0.65	>0.45[5]
Fraction Ar	0.05	0.51	0.22	–

[a] MW = molecular weight, HBA = number of hydrogen bond acceptors, HBD = number of hydrogen bond donors. [b] Ideal range based on guidelines of 'rule of three'.[3,16]

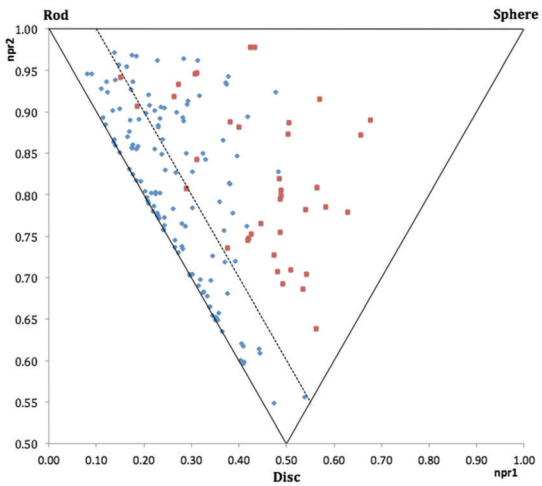

Fig. 2 Comparative PMI plot analysis of this work (red squares) and Maybridge diversity set 1 (blue diamonds). The three vertices of the triangular plot represent the extremes of molecular shape (rod, disc and sphere). npr = normalised PMI ratio.

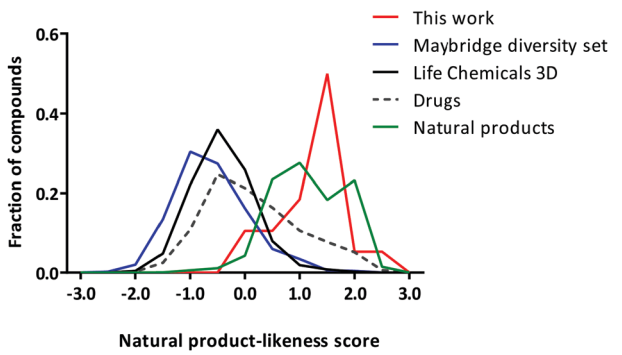

Fig. 3 NP-likeness analysis of this library, two commercially available fragment libraries, all FDA-approved drugs, and a collection of 2712 NPs (NuBBE) (logarithmic scale). Analysis was performed using the Natural-Product-Likeness Scorer.[18]

Thus, combined with the physicochemical analysis this data suggests the library to indeed be a NP-like fragment library.

In summary, challenges within FBDD have arisen with respect to the ease of elaboration of hits into potent lead compounds and the requirement for novel fragments. Herein, we have described a highly efficient approach for the synthesis of a library of 38 structurally diverse and complex small molecules based on 20 unique frameworks. Importantly, these fragments feature a high sp^3-content and polar functionality inspired by natural products to address the aforementioned hurdles. We also demonstrate the utility of the quaternary stereocentre as a further growth vector through the generation of alternative substituents and ring sizes. Importantly, the resultant library adheres to the 'rule of three' guidelines, thus demonstrating their suitability as a screening collection in this context.

We thank the EPSRC, BBSRC, Royal Society, Cambridge Trust, DTU, AstraZeneca, and the Carlsberg Foundation for funding. We also thank Dr H. F. Sore for discussions.

Conflicts of interest

There are no conflicts to declare.

Notes and references

1 C. W. Murray and D. C. Rees, *Nat. Chem.*, 2009, **1**, 187–192.
2 D. A. Erlanson, S. W. Fesik, R. E. Hubbard, W. Jahnke and H. Jhoti, *Nat. Rev. Drug Discovery*, 2016, **15**, 605–619.
3 C. W. Murray and D. C. Rees, *Angew. Chem., Int. Ed.*, 2016, **55**, 488–492.
4 M. M. Hann, A. R. Leach and G. Harper, *J. Chem. Inf. Comput. Sci.*, 2001, **41**, 856–864.
5 F. Lovering, J. Bikker and C. Humblet, *J. Med. Chem.*, 2009, **52**, 6752–6756.
6 T. J. Ritchie and S. J. F. Macdonald, *J. Med. Chem.*, 2014, **57**, 7206–7215.
7 B. Over, S. Wetzel, C. Grütter, Y. Nakai, S. Renner, D. Rauh and H. Waldmann, *Nat. Chem.*, 2013, **5**, 21–28.
8 (*a*) A. W. Hung, A. Ramek, Y. Wang, T. Kaya, J. A. Wilson, P. A. Clemons and D. W. Young, *Proc. Natl. Acad. Sci. U. S. A.*, 2011, **108**, 6799–6804; (*b*) D. J. Foley, P. G. E. Craven, P. M. Collins, R. G. Doveston, A. Aimon, R. Talon, I. Churcher, F. von Delft, S. P. Marsden and A. Nelson, *Chem. – Eur. J.*, 2017, **23**, 15227–15232.
9 (*a*) Y. Liu, S. J. Han, W. B. Liu and B. M. Stoltz, *Acc. Chem. Res.*, 2015, **48**, 740–751; (*b*) P. Hu, H. M. Chi, K. C. DeBacker, X. Gong, J. H. Keim, I. T. Hsu and S. A. Snyder, *Nature*, 2019, **569**, 703–707.
10 (*a*) C. J. Douglas and L. E. Overman, *Proc. Natl. Acad. Sci. U. S. A.*, 2004, **101**, 5363–5367; (*b*) H. Zheng, Y. Wang, C. Xu, X. Xu, L. Lin, X. Liu and X. Feng, *Nat. Commun.*, 2018, **9**, 1968.
11 J. Clardy and C. Walsh, *Nature*, 2004, **432**, 829–837.
12 (*a*) K. Mori and H. Mori, *Tetrahedron*, 1985, **41**, 5487–5493; (*b*) S. N. Ananchenko, Y. Y. Limanov, V. N. Leonov, V. N. Rzheznikov and I. V. Torgov, *Tetrahedron*, 1962, **18**, 1355–1367; (*c*) P. D. Thornton and D. J. Burnell, *Org. Lett.*, 2006, **8**, 3195–3198; (*d*) D. W. Brooks, P. G. Grothaus and W. L. Irwin, *J. Org. Chem.*, 1982, **47**, 2820–2821; (*e*) A. S. Chapelon, D. Moraléda, R. Rodriguez, C. Ollivier and M. Santelli, *Tetrahedron*, 2007, **63**, 11511–11616; (*f*) Y. Y. Yeung, R. J. Chein and E. J. Corey, *J. Am. Chem. Soc.*, 2007, **129**, 10346–10347; (*g*) G. J. Wu, Y. H. Zhang, D. X. Tan, L. He, B. C. Cao, Y. P. He and F. S. Han, *J. Org. Chem.*, 2019, **84**, 3223–3238.
13 G. Keserű, D. Erlanson, G. Ferenczy, M. Hann, C. Murray and S. Pickett, *J. Med. Chem.*, 2016, **59**, 8189–8206.
14 C. Baumgartner, S. Ma, Q. Liu and B. M. Stoltz, *Org. Biomol. Chem.*, 2010, **8**, 2915–2917.
15 W. Sauer and M. Schwarz, *J. Chem. Inf. Comput. Sci.*, 2003, **43**, 987–1003.
16 M. Congreve, R. Carr, C. W. Murray and H. Jhoti, *Drug Discov. Today*, 2003, **8**, 876–877.
17 (*a*) F. Lovering, *Med. Chem. Commun.*, 2013, **4**, 515–519; (*b*) A. D. Morley, A. Pugliese, K. Birchall, J. Bower, P. Brennan, N. Brown, T. Chapman, M. Drysdale, I. H. Gilbert, S. Hoelder, A. Jordan, S. V. Ley, A. Merritt, D. Miller, M. E. Swarbrick and P. G. Wyatt, *Drug Discovery Today*, 2013, **18**, 1221–1227.
18 K. Vanii Jayaseelan, P. Moreno, A. Truszkowski, P. Ertl and C. Steinbeck, *BMC Bioinf.*, 2012, **13**, 106.